

Integrated analysis of the expression profiles of the lncRNA-miRNA-mRNA ceRNA network in granulosa and cumulus cells from yak Ovaries

Ling Zhao

Gansu Agricultural University

Yangyang Pan

Gansu Agricultural University

Meng Wang

Gansu Agricultural University

Junqian wang

Gansu Agricultural University

Yaying Wang

Gansu Agricultural University

Xiaohong Han

Gansu Agricultural University

Jinglei Wang

Gansu Agricultural University

Tongxiang Zhang

Gansu Agricultural University

Tian Zhao

Gansu Agricultural University

Honghong He

Gansu Agricultural University

Yan Cui

Gansu Agricultural University

Sijiu Yu (✉ sijiuy@126.com)

Gansu Agricultural University

Research Article

Keywords: granulosa cells, cumulus cells, lncRNA, miRNA, ceRNA network

Posted Date: May 31st, 2022

DOI: <https://doi.org/10.21203/rs.3.rs-1661677/v1>

License: © ⓘ This work is licensed under a Creative Commons Attribution 4.0 International License.

[Read Full License](#)

Abstract

Background: Growing oocytes acquire the ability to mature through two-way communication between gametes and surrounding somatic cumulus cells (CCs). Granulosa cells (GCs) support oocyte growth, regulate meiosis progression, and modulate global oocyte transcription activity. However, the proliferation and differentiation of the yak ovary in GCs and CCs remain unclear. To characterize the important roles of lncRNAs, miRNAs, and mRNAs, whole-transcriptome analysis was performed. Real-time quantitative fluorescence PCR was performed to verify the selected RNA sequences.

Results: Important gene ontology terms and Kyoto Encyclopedia of Genes and Genomes pathways related to differentiation and oocyte development were identified for the target genes of differentially expressed lncRNAs, miRNAs, and mRNAs. In total, 6,223 mRNAs (2,197 upregulated, 4,026 downregulated), 643 lncRNAs (204 upregulated, 479 downregulated), and 559 miRNAs (311 upregulated, 248 downregulated) were significantly altered between the two groups; Target genes involved in cell adhesion, cell differentiation, regulation of developmental processes, cell proliferation, embryo development, signal transduction, apoptosis, and aromatic compound biosynthetic processes were significantly enriched. These RNAs were involved in ECM-receptor interaction, MAPK signaling, Hippo signaling, PI3K-Akt signaling, cell cycle, cell adhesion, leukocyte trans-endothelial migration, and actin cytoskeleton regulation.

Conclusions: A comprehensive analysis of the co-expression network of ceRNAs will facilitate the understanding of the process of granulosa cell proliferation and differentiation and offer a theoretical basis for the development of oocytes.

Background

In mammals, folliculogenesis and oogenesis occur in parallel within the ovary [1]. The ovarian follicle consists of an oocyte surrounded by theca and granulosa cells (GCs) involved in ovulation, fertilization, implantation, and embryo growth [2]. GCs preserve and breed oocytes and secrete steroid hormones, such as estrogen and progesterone, providing a crucial microenvironment for follicular growth [3]. Proliferation and differentiation of GCs is fundamental to the development of the follicle and the oocyte, to ovulation, and to luteinization, while apoptotic cell death performs the mechanism of ovarian follicle atresia. GCs are considered to maintain ovarian function. Growing oocytes in the ovary acquire the ability to mature through a two-way communication between the gamete and the surrounding somatic cumulus cells (CCs) [4–6]. Oocytes secrete a variety of growth factors to promote CC differentiation and proliferation [7]. These secreted molecules are mainly responsible for maintaining different stages of CCs and preventing their differentiation into membrane or granular cells [8].

Molecular replacement is the connection between the oocyte membrane and CCs through gap junctions [9]. Oocyte-granulosa cell communication is essential for the normal growth and development of both oocytes and follicles. Communication occurs via a bidirectional communication axis involving paracrine

signaling and the gap-junctional exchange of small regulatory molecules [10]. The genetic and transcriptional characteristics of the cumulus-oocyte complex (COC) are reflected in the developmental potential for successful fertilization and embryonic development. However, little is known about the relationship between genes expressed in oocytes and CCs [11]. Studies that analyze the transcriptome of GCs and CCs may be a powerful tool to improve our knowledge of the pathways involved in oocyte development. Microarray technology has enabled the discovery of many ontological groups that are closely or loosely associated with oocyte development, CCs and GCs proliferation, and apoptosis.

This study aims to explore the markers of GCs and CCs that participate in the development of oocytes and affect cell proliferation, migration, and apoptosis. Yak GCs and CCs were cultured in vitro. Transcriptome changes in granulosa and cumulus cell genes are involved in regulating cell migration, cell proliferation, and programmed cell death. Genes that were significantly different in the granulosa and cumulus cell types were analyzed. Our results provide evidence on the proliferation and differentiation of GCs and CCs and can identify genes related to oocyte development.

A new mechanism of interaction between non-coding RNA and mRNA has been proposed, in which long non-coding RNAs (lncRNAs), messenger RNAs (mRNAs), and micro RNAs (miRNAs) are involved [12]. lncRNAs play a key role in many biological processes, including cell cycle regulation, epigenetic changes, and dose compensation [13]. Studies have shown that lncRNAs can also be used as competitive endogenous RNA (ceRNAs), which act as miRNA sponges, and participate in regulating the expression of target genes [14, 15]. miRNAs can negatively regulate protein-coding genes by combining them with complementary sequences [16]. lncRNAs and miRNAs affect ovarian growth, cell proliferation, aging, and apoptosis [17]. In regulatory ceRNA networks, lncRNAs and miRNAs coordinate to integrate and regulate various aspects of ovarian tissue development. Although lncRNAs do not encode proteins, they have been shown to have transcriptional and post-transcriptional effects on gene function, because they usually participate in different physiological processes [18]. lncRNAs and miRNAs play an important role in regulating ovarian maturation, ovarian cell development, and hormone secretion [19].

Therefore, the integration of lncRNAs and miRNAs can be used to study the regulatory mechanisms underlying ovarian growth at the molecular level [17]. In the current study, we analyzed the expression profiles of lncRNAs, mRNA, and miRNAs in GCs and CCs cultured in vitro for two generations. Whole-transcriptome analysis revealed additional molecular changes. These data will help to further understanding of this mechanism on the influence of oocyte development.

Methods

Sample Collection

Yak ovary samples were obtained from a local commercial slaughterhouse in Xining City, Qinghai Province, China. After learning about the sanitation and related conditions of the slaughterhouse, we entered it to collect yak ovaries. After the yak was slaughtered, the ovaries containing antral follicles were

picked, washed with sterile normal saline, and then stored for 4°C, and quickly returned to the laboratory. A total of 477 samples were collected, of which 150 were used to collect GCs, and 327 were used to collect CCs. GCs and CCs were cultured in vitro and samples of GCs and CCs were harvested for RNA extraction, put into an Eppendorf tube without RNase, and immediately stored in liquid nitrogen. All samples were stored at - 80°C until analysis.

In vitro culture of yak granulosa cells and cumulus cells

The obtained follicular fluid was injected into a 15 mL centrifuge tube containing 2 mL of PBS, the follicular fluid was gently pipetted and mixed, 1000 rpm for 5 min, the supernatant was discarded, 5 mL of DMEM/F12 and 10% FBS to wash the cells into a single suspension, and the trypan blue exclusion method was used. Check the cell viability. The remaining cell fluid was washed again by centrifugation. Discard the culture medium, add an appropriate amount of cell culture medium, adjust the cell density to 5×10^5 , and inoculate it in a cell flask or petri dish, then place it in a 5% CO₂, 37 °C incubator for culture, observe the cells under an inverted phase contrast microscope and record the growth situation by photographing (Olympus CK41, Tokyo, Japan).

LncRNA and mRNA Sequencing and Data Processing

Total RNA was extracted using a TRIzol reagent kit (Invitrogen, Carlsbad, CA, USA) according to the manufacturer's protocol. RNA quality was assessed using an Agilent 2100 Bioanalyzer (Agilent Technologies, Palo Alto, CA, USA) and verified by RNase-free agarose gel electrophoresis. Ribosomal RNAs (rRNAs) were then removed to retain mRNAs and ncRNAs using the epicenter RiboZero™ reagent, and the remaining RNAs were randomly fragmented into short fragments that were used for cDNA synthesis. We performed library construction using a strand-specific method according to the following steps: First-strand cDNA was synthesized using random hexamers with rRNA-depleted RNA as template. dNTPs, RNase H, and DNA polymerase I were used for second-strand synthesis. The cDNA was purified using AMPure XP beads. Next, cDNA fragment purification, end repair, poly(A) addition, and Illumina sequencing adapter ligation were carried out using the QIAquick PCR extraction kit. Then UNG (Uracil-N-Glycosylase) was used to digest the second-strand cDNA. cDNA fragments were size-selected by agarose gel electrophoresis, PCR-amplified, and sequenced using Illumina HiSeq™ 4000 by Gene Denovo Biotechnology Co. (Guangzhou, China).

Raw reads were first quality filtered by Fastp (V0.18.0) [20] to remove reads containing less than 10% unknown nucleotides (N) and low-quality reads (> 50% bases, qvalue \leq 20) and generate clean reads. All downstream analyses are performed based on high quality cleaning data. Bowtie2 (V2.2.8) [21] was used to map reads to a ribosomal RNA (rRNA) database. Clean, paired-end reads were mapped to the reference genome using HISAT2 (V2.1.0) [22] with the significance of differentially expressed lncRNAs and mRNAs was analyzed using the R package DESeq2 [23], and p-values < 0.05, and fold-change > 2 were the filtering criteria to identify significant DEGs. Mapped reads from each library are assembled by StringTie (V1.3.4) [24]. Differential expression pattern clustering was then performed using the Gene Denovo platform. Expression levels of lncRNA and mRNA were normalized using FPKM (fragment of transcript per million

mapped reads per kilobase). The CNCI[25], CPC[26], PFAM[27] and CPAT[28] were used to analyze the coding potential of the transcripts. The assembled transcripts, without the coding potential of their overlap, were the candidate set of lncRNAs. The reference genome and gene model annotation files of the yak (BosGru v2.0, https://www.ncbi.nlm.nih.gov/assembly/GCF_000298355.1/) were downloaded directly from the genome website.

Library Construction and miRNA

Sequencing the RNA molecules in a size range of 18–30 nt were enriched using polyacrylamide gel electrophoresis (PAGE). Then, the 3' adapters were added and the 36–44 nt RNAs were enriched. The 5' adapters were then ligated to the RNAs. The ligation products were reverse-transcribed by PCR amplification and the 140–160 bp size PCR products were enriched to generate a cDNA library. To obtain a clean label, we filtered the original reading by:

Removing low quality reads;

Removing reads without 3' adapters;

Removing reads containing 5' adapters;

Removing reads containing poly A in small RNA fragment;

Removing reads shorter than 18 nt;

Removing reads containing 3' and 5' adapters, but no small RNA fragments between them.

All clean tags were aligned with the reference genome and then searched against the miRBase database [29] (Release 22) to identify known yak miRNAs. After excluding the reads mapped to known miRNA/ncRNA/repeat regions/mRNA regions, all unannotated tags were aligned with the reference genome. According to their genome positions and hairpin structures predicted by software Mireap_v0.2 (<https://sourceforge.net/projects/mireap/>), the novel miRNA candidates were identified. Transcripts per million (TPM) was used to determine miRNA expression levels.

Differentially Expressed lncRNA, miRNA and mRNA

Differentially expressed transcripts across samples or groups were identified as mRNA and lncRNA with a fold-change ≥ 2 and a false discovery rate (FDR) < 0.05 , and miRNAs with a fold-change ≥ 2 and $p < 0.05$, in a comparison as significant DE lncRNA, DE miRNA, and DE mRNA by DESeq2 [23] or edgeR package [30].

Construction of the ceRNA Network

Competitive endogenous RNAs (ceRNAs) are transcriptional regulators that modulate the expression of transcripts through competitive binding. The miRNA-mRNA and miRNA-lncRNA interactions were predicted using TargetScan and miRanda, and the competitive pairs of mRNA-lncRNA were identified

using a hypergeometric test and Pearson's correlation coefficient. Based on the sharing of miRNA binding sites and competitive pairs between lncRNAs and mRNAs, a ceRNA network was constructed as follows: $P < 0.01$, $FDR < 0.01$, in the hypergeometric test [31–33]. Visualization of ceRNA was performed using the Cytoscape software (<http://cytoscape.org/>).

Spearman's rank correlation coefficient between miRNA and candidate ceRNA was calculated for target gene pairs, and target gene pairs with correlation coefficients less than or equal to -0.7 were screened. The ceRNA theory believes that the expression levels of ceRNAs competing for the same miRNA are positively correlated, so we calculated the Pearson correlation coefficient for the expression levels between the ceRNA pairs obtained in the previous step, and selected the ceRNA pairs with a correlation coefficient of more than 0.9. Based on the above threshold screening, and then using the hypergeometric distribution test [34], the ceRNA pairs with a P value < 0.05 were screened as the final ceRNA pairs.

Expression Analysis of DE lncRNA, DE miRNA, and DE Genes Using RT-qPCR

Primers were designed according to transcriptome sequencing data for CC and GC using Primer Premier 6.0. RT-qPCR was performed on 12 DE mRNAs, 12 DE lncRNAs, and 8 DE miRNAs selected from RNA-seq data according to their latent functional importance. First-strand cDNA was synthesized using the Evo M-MLV RT Kit with gDNA clean for qPCR (Accurate Biotechnology, Hunan, China). RT-qPCR was performed on each sample in triplicate using the SYBR Green Premix Pro Taq HS qPCR Kit (Accurate Biotechnology, Hunan, China) on a LightCycler®480 Instrument II (Roche, Switzerland) in a 20 μ L reaction volume. The cycling parameters for the PCR amplification were as follows: 95°C for 30 s, followed by 40 cycles at 95°C for 5s and 60°C for 30 s (Table 1–3). Amplification specificity was evaluated using melting curve analysis. The relative expression of target gene transcripts was calculated using the comparative Ct method ($2^{-\Delta\Delta C_t}$) and subjected to statistical analysis using the SPSS software (version 19).

Table 1

RT-qPCR primers of mRNA for cumulus cells and Granulosa cells

Gene	Transcript ID	Primer sequences (5'-3')	Product Size(bp)
RAC1	ncbi_102273253	F: CCCAACACACCCATCATC R: TCGCCTCATCAAACACTG	202
CDKN1A	ncbi_102268672	F: ACTTGGACCTGTCGCTGT R:GGAGTGGTAGAAATCTGTCAT	131
VEGFA	ncbi_102270607	F: GGCTGCTGTAATGACGAA R: TCTCCTATGTGCTGGCTT	104
ITGB1	ncbi_102273972	F: AGACGACTTGGAGAATGTG R: GCTGGTGTGCTGCTAATG	135
SGK1	ncbi_102272039	F: AGTTGTTCTACCATCTCCAG R: CGTTGTGCCATTGTGTTC	215
FGFR4	ncbi_102267813	F:CCACCACATTGACTACTACA R: TCCAAACGACCACACATC	118
JAK3	ncbi_102286011	F: CGGATGATGGGATGTGAG R: AATGATGGTCGGTCTTGAG	158
NR4A1	ncbi_102288141	F: GGAGGTGATTCGCAAGTG R: CCAGACGGAGGATAAAGAG	113
ITGA6	ncbi_102265941	F:AAGATGATATGGATGGAGGAG R: AACGCAATGTAATGGAAGTC	124
LAMA5	ncbi_102266736	F: GTGGTGTCCCTTGGTGAAC R: GCTGATGTCCTTGATACTGT	195
AKT3	ncbi_102265427	F: GCCTTGGACTATCTACATTC R: CCCGCACATCATTTCATAC	255
CCND1	ncbi_102270546	F: CGAGGAGAACAAGCAGAT R: GCGGTGATAGGAGAGGAA	172
β -actin	NM_173979.3	F: CCGTGACATCAAGGAGAAG R: AGGAAGGAAGGCTGGAAG	174

Table 2
RT-qPCR primers of LncRNA for cumulus cells and Granulosa cells

Types	Transcript ID	Primer sequences (5'-3')
	MSTRG.17330.1	F: GAAGGCAGGAGAAGAAGG
LncRNA	(PHLPP1)	R: GAACCAGGACCAGAATGAG
	XR_001351765.1(TEK)	F: CCTCTCTAAATACCTGGAACC
	MSTRG.1083.1	R: AACACCTTACACGATAGCC
	(PCGF6)	F: GGCTTCTCTGGTGGTTCA
	MSTRG.8701.9	R: AGGGTAGATGGGCTGGAA
	(MDM4)	F: GACCTTGCTTGCTTGGAA
	MSTRG.13933.1	R:CACAGACTTAGAGAACTTACAG
	(ID2)	F: TGTGCGGGATTACTTTGC
	MSTRG.12026.1	R: AGGCTGACTGGACTCTGA
	(SMURF1)	F: CAAGACAGGAAGCCAGTG
	MSTRG.1083.1	R: CAGATACAAACCCAGGAGTG
	(PCGF6)	F: GCAAGGAGAAGTGAGGATT
	MSTRG.17464.1	R: CTGAGCGTGAAGAGGAAG
	(PRKAR1B)	F: ATGGCTGAACTCAAGTCC
	MSTRG.919.1	R: TGGGTTTCTCCTGTTGTG
	(CDKN2A)	F: CGCTACGCTCCACTTCTA
	MSTRG.13216.1	R: CACTTCAGGTTCTCACAGG
	(Pol)	F:GAGGAGAAGAGGAGGAGAG
	MSTRG.3682.1	R: TGGCAGGAAGTCAGAGATA
	(PAOX)	F: AAGAGATGGAAGGACTGG
	MSTRG.9809.1	R: GACTGAACAAGGGCATTT
	(LOC102277897)	F: TGCGACTTCACTTTCACTT
		R: CAGATACAGGAGCCAGGAT

Table 3
RT-qPCR primers of miRNA for cumulus cells and Granulosa cells

Types	Transcript ID	Primer sequences (5'-3')
	miR-2431-y	F: CACCCCACTTGCATGACCCTGA
	miR-7977-X	F: TTCCCGGCCAACGCACCA
miRNA	miR-2284-Z	F: AAAAAGTTCGTTTGGGTTTTCT
	miR-365-y	F: TAATGCCCTAAAAATCCTTAT
	miR-7862-y	F: TGGTGCTCCCTGGAGCTGAGC
	miR-342-y	F:TCTCACACAGAAATCGCACCCATC
	miR-195-X	F: TAGCAGCACAGAAATATTGGCA
	miR-574-X	F: TGAGTGTGTGTGTGTGAGTGTGT
	U6(XM_021614042.1)	F: GGAACGATACAGAGAAGATTAGC R: TGGAACGCTTCACGAATTTGCG

Results

Morphology of the Granulosum Cell and Cumulus Cell

An inverted phase contrast microscope showed that the flat primary GCs displayed typical epithelioid-like growth and the cells had a clear nuclear boundary; the cells were polygonal or irregular polygonal stellate cells, tightly connected, and intact and in good condition (Fig. 1A). After 48 h of culturing primary CCs in vitro, they adhered to the wall and grew from a round shape to a long spindle shape, extending at both ends, and there were large gaps between the cells. When the cells grew to approximately 90% confluency, they became irregular polygons, with stable shapes, long spindles, and the occasional regular polygon (Fig. 1B).

Overview of RNA-seq Results in Granulosa Cells and Cumulus Cells

Six cDNA libraries, including three from the cumulus cell group (CC: CC-1, CC-2, and CC-3) and three from the granulosa cell group (GC: GC-1, GC-2, and GC-3), were constructed and analyzed by high-throughput sequencing. A total of 77.076 G clean bases were obtained and deposited in the National Center for Biotechnology Information database under accession number SRP307630. After quality control and filtering the raw reads, 512, 524, and 562 high-quality clean reads were generated from the six libraries. The comparison software Bowtie2 (version 2.2.8) was used to compare high-quality clean reads to the ribosome of the species (mismatch number: 0) and to remove the reads corresponding to ribosomal RNA, and 511,825,690 effective reads were obtained. The average Q30 was 91.765% and the average GC

content was 48.636%. Ribosomal RNA reads were filtered based on the updated reference genome of yak [35] and the majority of effective reads were successfully mapped; the average mapped ratio was 92.34%. The differentially expressed genes (DEGs) analysis based on the genome was reliable.

Differential Expression Analysis of DE LncRNAs, DE mRNAs and DE miRNAs

A total of 1,411 lncRNAs were obtained from the six libraries, and 643 significantly differentially expressed (DE) lncRNAs were identified by a false discovery rate (FDR) < 0.05 , and $|\log_2(\text{fold-change})| \geq 1.0$, among which 204 DE lncRNAs were upregulated, and 439 DE lncRNAs were downregulated (Fig. 2A, Table S4). The total DE lncRNAs are presented as a heatmap based on gene expression (Fig. 3A). A total of 20,519 mRNAs and 6,223 significantly differentially expressed mRNAs were identified, among which 2,197 DE mRNA were upregulated and 4,026 DE mRNA were downregulated (Fig. 2B, Table S5). Total DE mRNA is presented as a heat map based on gene expression (Fig. 3B). Additionally, a total of 2,248 miRNAs and 559 DE miRNAs were identified by stringent thresholds (FDR < 0.05), among which 311 DE miRNAs were upregulated, and 248 DE miRNAs were significantly downregulated between the two groups (Fig. 2C, Table S6). The total DE miRNAs are presented in a heat map based on gene expression (Fig. 3C).

Regulatory ceRNA Network (DE lncRNA-DE miRNA-DE mRNA) of CCs and GCs

We performed gene ontology (GO) enrichment and Kyoto Encyclopedia of Genes and Genomes (KEGG) enrichment analysis of DE mRNAs. GO enrichment analysis revealed that these DE mRNA were significantly enriched in some target genes involved in cell adhesion, cell differentiation, regulation of developmental processes, cell proliferation, embryo development, regulation of signal transduction, programmed cell death, and aromatic compound biosynthetic process (Fig. 4, 6A, Table S7). The ordinate represents a GO term. The abscissa represents the enrichment factor. The number of differences in this GO term is divided by all the numbers, and size indicates the number; the redder the color, the smaller the P/Q value. KEGG enrichment analysis showed that these target genes were significantly enriched in many pathways, including leukocyte trans-endothelial migration ECM-receptor interaction, MAPK signaling, Hippo signaling, cell cycle, cell adhesion, PI3K-Akt signaling, and regulation of the actin cytoskeleton (Fig. 5, 6B, Table S8) The X-axis indicates the detailed terms. The Y-axis indicates the gene numbers.

We set the parameters according to the gradient method and found that the negative correlation was < -0.95 , the positive correlation was > 0.95 , and when $P < 0.01$, there were a total of 540 relationship pairs. The constructed a mini-ceRNA (DE lncRNA-DE miRNA-DE mRNA) network of important RNAs (Fig. 7A, Table S9). Therefore, we constructed a ceRNA network in which the network diagram of mRNA-miRNA-lncRNA was drawn using Cytoscape, in which the mRNA is represented by circles, miRNA triangles, and lncRNA diamonds. During the analysis, it was found that according to the process parameters: negative correlation ≤ -0.7 , positive correlation ≥ 0.9 , and P value < 0.05 , there were a total of 53,034 relationship pairs, so many relationship pairs could not be presented through a network diagram.

Among them, three mRNAs with significant differences were screened, their related lncRNA and miRNA relationship pairs were selected, and a correlation network map was constructed. The subnetworks of ncbi_102270546 (CCND1) are displayed (Fig. 7B, Table S10), which shows that CCND1 expression is regulated by 31 miRNAs and 66 lncRNAs. Among them, the most significant differences were observed in MSTRG.13544.2 and miR-221-x|miR-2357-x|miR-338-y|novel-m0707-5p. The subnetworks of ncbi_102265941 (ITGA6) and ncbi_102268672 (CDKN1A) are shown (Fig. 7C, D and Table S10), respectively. The target gene ITGA6 was regulated by 12 miRNAs and 84 lncRNAs, and the relationship pairs with significant differences were MSTRG.9576.6-miR-11987-x|miR-2284-y|novel-m0070-3p|novel-m0191-3p-ncbi_102265941. In addition, CDKN1A was regulated by 12 miRNAs, 29 lncRNAs, and the differentially significant relationship pairs: MSTRG. 5969.1-novel-m0122-5p | novel-m5969-3p-ncbi102268672.

We identified 12 known mRNAs related to cell proliferation, differentiation, and regulation of signal transduction and cell adhesion, as well as cell growth, death, and regulation of cyclin. Some target genes are involved in cell adhesion, cell differentiation, regulation of developmental processes, cell proliferation, embryo development, signal transduction, programmed cell death, and aromatic compound biosynthetic processes. These RNAs are involved in many pathways, including leukocyte trans-endothelial migration, ECM-receptor interaction, the MAPK signaling pathway, the Hippo signaling pathway, the cell cycle, cell adhesion, the PI3K-Akt signaling pathway, and regulation of the actin cytoskeleton.

Validation of DE lncRNA, DE miRNA and DE mRNA Expression by RT-qPCR

The relative expression (log₂FC) of these DEGs was similar between the two approaches, although some quantitative differences were found between the RT-qPCR and RNA-seq analytical platforms (Fig. 8). Therefore, the RNA-seq results were reliable and could be used for bioinformatic analysis.

Discussion

The ovary is the female gonad that is present as a pair in most animals and is responsible for the generation of female gametes and the production of hormones that regulate reproductive functions. The growth and development of mammalian oocytes occurs in a specialized compartment of the ovary called the follicle. Follicle development in mammals mainly includes primordial, primary, secondary, tertiary, and mature follicle stages. Primordial follicles are composed of a single flat layer of GCs surrounded by immature oocytes. Further differentiation of primary follicles into preantral follicles involves acquisition of a theca layer around the GC layer and GC division through mitosis to form multiple layers of GCs (the theca layer remains as a single layer at this stage). The growth and development of oocytes affect the functional activities of surrounding somatic cells [36]. The interaction between oocytes and surrounding somatic cells progresses as the oocyte is released from the state of quiescence toward ovulation, fertilization and zygote formation. As follicles grow and cavities form, somatic cells are divided into two distinct subtypes: the CCs, which surround and are in close metabolic contact with the oocyte, and the

parietal GCs, which are follicle-forming cells [37]. Numerous factors affect oocyte developmental capacity and granulosa cell and follicular microenvironment changes, including heat stress [38]. GCs are tightly connected to oocytes in mammalian ovaries through gap junctions and provide oocytes with the essential signals and metabolites required for oocyte growth and maturation [39]. CCs support meiotic arrest and cytoplasmic maturation of the oocyte by exporting cyclic adenosine nucleotides [40], calcium [41], other metabolites [42], and unknown signals that control transcription in the occluded oocyte [43].

Proper folliculogenesis and ovulation can only be achieved through reciprocal signaling events generated by intimate granulosa cell-oocyte communication [44]. Before ovulation, differentiated GCs can secrete a large amount of sex hormones and growth factors in follicles to ensure successful ovulation [45]. The functions of the two different cells in the whole follicle development process are not consistent: CCs play a key role in the normal growth and development of oocytes, while GCs mainly play an endocrine function to support the growth of the follicle [8]. After ovulation, GCs undergo terminal differentiation into luteal cells and continue to play an endocrine role, while CCs and co-ovulate with oocytes to assist in egg retrieval and the sperm acrosome reaction. Although some functional differences between these two types of follicular somatic cells have been well described, it is not clear which genes regulate their developmental pathways. Previous studies have found that the ability of oocytes to promote follicular cell proliferation was first directly demonstrated in mice [46].

GC proliferation, steroid production, and morphological changes are primarily linked to molecular pathways. Sheep GCs overexpress the sonic hedgehog (Shh) signaling pathway, which has the same potential role as the Hedgehog pathway in increasing GCs proliferation at the preantral stage [47]. An important factor in maintaining follicle and oocyte growth for reproductive success is proper regulation of granulosa cell activity [48]. In the ovary, the β -catenin-dependent canonical pathway of WNT4 leads to an ovarian-dependent pathway. WNT proteins can also signal through Rho-GTPases, utilizing non-canonical pathways associated with changes in polarized cell shape and migration [49]. This ameliorates small changes in cell shape that affect GCs during early folliculogenesis. The study uncovered two classes of cellular interactions, demonstrating a complex dialogue between compartments: molecular dialogue (signaling pathways) and physical communication (gap junctions and trans-regional projections) [50].

lncRNAs are more than 200 nucleotides in length and constitute a family of transcripts that are unable to encode protein [51]. This theory suggests that lncRNAs act as natural sponges or decoys to competitively bind certain miRNAs and reduce the binding of miRNAs to corresponding target genes, resulting in altered miRNA target gene expression [52, 53]. However, it remains unclear whether abnormal lncRNAs exert ceRNA effects on some miRNAs and exert certain effects on signal transduction during cell proliferation and differentiation by indirectly regulating the expression of target mRNAs.

In this study, a total of 1,411 lncRNAs and 643 significantly DE lncRNAs were obtained from the six libraries, of which 204 DE lncRNAs were upregulated and 439 DE lncRNAs were downregulated. A total of 20,519 mRNAs and 6,223 significantly differentially expressed mRNAs were identified, among which 2,197 DE mRNAs were upregulated and 4,026 DE mRNA were downregulated. Additionally, a total of

2,248 miRNAs and 559 significantly differentially expressed miRNAs were identified, among which 311 DE miRNAs were upregulated, and 248 DE miRNAs were downregulated significantly between the two groups. Some target genes are involved in cell adhesion, cell differentiation, regulation of developmental processes, cell proliferation, embryo development, signal transduction, programmed cell death, and aromatic compound biosynthetic processes. These RNAs were involved in many processes and pathways, including leukocyte trans-endothelial migration, ECM-receptor interaction, the MAPK signaling pathway, the Hippo signaling pathway, the cell cycle, cell adhesion, the PI3K-Akt signaling pathway, and regulation of the actin cytoskeleton. Few lncRNAs showed clear spatiotemporal expression and specificity in the process of tissue growth and differentiation.

Cyclin D1 is encoded by the CCND1 gene located on chromosome band 11q13 and promotes cell cycle progression during the G1-S phase [54]. Activation of the PI3K/Akt pathway promotes an up-regulation mechanism of CCND1, in which mTor can activate CCND1 translation and promote the synthesis of cyclin D1/CDK4 and CDK6 complexes involved in cell cycle progression [55]. Amplification of CCND1 is prevalent in human cancers. Dai et al propose a role for CCND1 in promoting ovarian cancer cell proliferation, which could be alleviated by treatment [56]. CDKN1A encodes P21 and is a cyclin-dependent kinase (Cdk) inhibitor [57]. In cancer cell lines, p21 acts as an activator to synthesize and activate cyclin D/Cdk4 or Cdk6 complexes to enhance proliferation efficiency [58], and hyperphosphorylated p21 activates Cdk1 upon G2/M transition [59]. p21 is both an inhibitor and activator of the cell cycle, depending on the cellular environment and its expression levels. In contrast, p21 is involved in checkpoint control and initiates temporary cell cycle arrest. [60]. Interestingly, we also enriched the network graph for ITGA6. When ITGA6 forms $\alpha 6\beta 1$ and $\alpha 6\beta 4$ integrin complexes with other integrin subunits, embryogenesis, organogenesis, and cancer cell invasion can be mediated [61]. From these differential genes, we will provide more predictive target genes for the differentiation of GCs and CCs.

Little research has been conducted to explore the mechanism of lncRNAs in GCs and CCs. The present study had several strengths. We constructed a ceRNA network in which a network diagram of mRNA-miRNA-lncRNA was drawn. There were 540 relationship pairs, which provided a reference for exploring biological processes such as proliferation, differentiation, and signal transduction between CCs and GCs. The evidence we provide here suggests that differential mRNA-miRNA-lncRNA may play an important role in follicle development and ovulation. However, the specific mechanism requires further exploration in cell and animal experiments.

Conclusions

In conclusion, this study systematically characterized the ceRNA regulatory network and biochemical parameters of CCs and GCs. Many identified lncRNAs, miRNAs, and mRNA provide a reference for further research on the regulatory mechanisms of ceRNAs. Our findings also provide new insights into the molecular mechanisms of CCs and GCs proliferation, differentiation, and signal transduction, which will help explore the effects of CCs and GCs on follicle growth and oocyte development.

Abbreviations

CCs: Cumulus cells; GCs: Granulosa cells; GO: Gene Ontology; RT-qPCR: Quantitative real-time PCR; KEGG: Kyoto Encyclopedia of Genes and Genomes; DMEM: Dulbecco's modified Eagle's medium; FBS: Foetal bovine serum; PBS: Phosphate buffered saline

Declarations

Institutional Review Board Statement

The experimental protocol was reviewed and approved by the Faculty of Animal Veterinary Medicine, Gansu Agricultural University (approval number GSAU-Eth-VMC-2022-018) and performed in agreement with the Care and Use Guidelines of Experimental Animals published by the Ministry of Science and Technology of the People's Republic of China.

Ethics approval and consent to participate

The experimental protocol was reviewed and approved by the Faculty of Animal Veterinary Medicine, Gansu Agricultural University (approval number GSAU-Eth-VMC-2022-018) and performed in agreement with the Care and Use Guidelines of Experimental Animals published by the Ministry of Science and Technology of the People's Republic of China.

Consent for publication

Not applicable.

Availability of data and materials

Raw sequencing reads of lncRNA-seq and miRNA-seq in this paper have been deposited in the NCBI Sequence Read Archive (SRA) under BioProject accession number PRJNA704089

Competing interests

The authors declare no conflict of interest.

Funding

This research was funded by the National Natural Science Foundation of China (32160859, 31972760), the Prominent Youth Foundation of Gansu Province (20JR10RA561), Major Science and Technology Project of Gansu Province (21ZD10NA001), and the Seed Industry Research Project of Gansu Province (GZGG-2021-1).

Authors' contributions

Conceptualization, Y.P. and L.Z.; methodology, M.W. and L.Z.; software, L.Z. and J.W.; validation, X.H. and Y.W.; formal analysis, L.Z., T.Z. and J.W.; investigation, L.Z., Y.P. and M.W.; resources, L.Z., Y.C., J.W. and T.Z.; data curation, L.Z., J.W. and H.H.; writing original draft preparation, L.Z.; writing review and editing, Y.P. and S.Y.; visualization, L.Z., M.W. and Y.C.; supervision, S.Y.; project administration, S.Y. and L.Z.; funding acquisition, S.Y. All authors have read and agreed to the published version of the manuscript.

Acknowledgments

We thank the local commercial slaughterhouse in Xining City, Qinghai Province for providing the experimental animals.

References

1. Sheldon IM, Noakes D, Dobson H: **The influence of ovarian activity and uterine involution determined by ultrasonography on subsequent reproductive performance of dairy cows.** *Theriogenology* 2000, **54**(3):409–419. <https://pubmed.ncbi.nlm.nih.gov/11051324/> PMID: 11051324
2. Macklon NS, Fauser B: **Aspects of ovarian follicle development throughout life.** *Hormone Research* 2000, **52**(4):161–170. <https://pubmed.ncbi.nlm.nih.gov/10725781/> PMID: 10725781
3. Vanderhyden, Telfer, Eppig: **Mouse oocytes promote proliferation of granulosa cells from preantral and antral follicles in vitro.** *Biology of reproduction* 1992. <https://pubmed.ncbi.nlm.nih.gov/1391318/> PMID: 1391318
4. Kempisty B, Ziółkowska A, Ciesiółka S, Piotrowska H, Antosik P, Bukowska D, Nowicki M, Brüßow KP, Zabel M: **Study on connexin gene and protein expression and cellular distribution in relation to real-time proliferation of porcine granulosa cells.** *Journal of biological regulators and homeostatic agents* 2014, **28**(4):625–635. <https://pubmed.ncbi.nlm.nih.gov/25620173/> PMID: 25620173
5. Diaz FJ, Wigglesworth K, Eppig JJ: **Oocytes are required for the preantral granulosa cell to cumulus cell transition in mice - ScienceDirect.** *Developmental Biology* 2007, **305**(1):300–311. <https://pubmed.ncbi.nlm.nih.gov/17368609/> PMID: 17368609 PMCID: PMC1899534
6. Rybska M, Knap S, Jankowski M, Jeseta M, Bukowska D, Antosik P, Nowicki M, Zabel M, Kempisty B, Ja?Kowski JM: **Cytoplasmic and nuclear maturation of oocytes in mammals – living in the shadow of cells developmental capability.** *Medical Journal of Cell Biology*, **6**(1). <https://doi.org/10.2478/acb-2018-0003> DOI: 10.2478/acb-2018-0003
7. Gilchrist RB, Ritter LJ, Armstrong DT: **Oocyte–somatic cell interactions during follicle development in mammals.** *Animal Reproduction Science* 2004, **82**(none):431–446. <https://pubmed.ncbi.nlm.nih.gov/15271471/> PMID: 15271471
8. Li, R.: **Oocyte-secreted factor(s) determine functional differences between bovine mural granulosa cells and cumulus cells.** *Biology of Reproduction* 2000, **63**(3):839–845. <https://pubmed.ncbi.nlm.nih.gov/10952929/> PMID: 10952929

9. Macaulay AD, Gilbert I, Caballero J, Barreto R, Fournier E, Tossou P, Sirard MA, Clarke HJ, Khandjian EW, Richard FJ: **The gametic synapse: RNA transfer to the bovine oocyte.** *Biology of Reproduction* 2014, **91**(4):90. <https://pubmed.ncbi.nlm.nih.gov/25143353/> PMID: 25143353
10. Sutton ML, Gilchrist RB, Thompson JG: **Effects of in-vivo and in-vitro environments on the metabolism of the cumulus-oocyte complex and its influence on oocyte developmental capacity.** *Hum Reprod Updat* 2003(1):35–48. <https://pubmed.ncbi.nlm.nih.gov/12638780/> PMID: 12638780
11. Biase FH, Kimble KM: **Functional signaling and gene regulatory networks between the oocyte and the surrounding cumulus cells.** *Bmc Genomics* 2018, **19**(1). <https://pubmed.ncbi.nlm.nih.gov/29747587/> PMID: 29747587 PMCID: PMC5946446
12. Salmena L, Poliseno L, Tay Y, Kats L, Pandolfi PP: **A ceRNA hypothesis: The rosetta stone of a hidden RNA language?** *Cell* 2011, **146**(3):353–358. <https://pubmed.ncbi.nlm.nih.gov/21802130/> PMID: 21802130 PMCID: PMC3235919
13. Spizzo R, Almeida MI, Colombatti A, Calin GA: **Long non-coding RNAs and cancer: a new frontier of translational research?** *Oncogene* 2012, **31**(43):4577–4587. <https://pubmed.ncbi.nlm.nih.gov/22266873/> PMID: 22266873 PMCID: PMC3433647
14. Xiaoli, Kong, Duan, Yuting, Sang, Yaming, Hanwen, Zhang, Yiran, Liang: **LncRNA-CDC6 promotes breast cancer progression and function as ceRNA to target CDC6 by sponging microRNA-215.** *Journal of cellular physiology* 2018. <https://pubmed.ncbi.nlm.nih.gov/30362551/> PMID: 30362551
15. Paraskevopoulou M, Hatzigeorgiou AG: **Analyzing MiRNA–LncRNA Interactions:** *Methods Mol Biol*; 2016. <https://pubmed.ncbi.nlm.nih.gov/26721498/> PMID: 26721498
16. Fabian MR, Sonenberg N, Filipowicz W: **Regulation of mRNA translation and stability by microRNAs.** *Annual Review of Biochemistry* 2010, **79**(1):351–379. <https://pubmed.ncbi.nlm.nih.gov/20533884/> PMID: 20533884
17. Miao X, Luo Q, Zhao H, Qin X: **Genome-wide analysis of miRNAs in the ovaries of Jining Grey and Laiwu Black goats to explore the regulation of fecundity.** *Scientific Reports* 2016, **6**:37983. <https://pubmed.ncbi.nlm.nih.gov/27897262/> PMID: 27897262 PMCID: PMC5126701
18. Liu KS, Li TP, Hua T, Mao XD, Chen YJ: **Advances of Long Noncoding RNAs-mediated Regulation in Reproduction.** *Chinese Medical Journal* 2018, **131**(2):226–234. <https://pubmed.ncbi.nlm.nih.gov/29336373/> PMID: 29336373 PMCID: PMC5776855
19. Miao X, Luo Q, Zhao H, Qin X: **An Integrated Analysis of miRNAs and Methylated Genes Encoding mRNAs and lncRNAs in Sheep Breeds with Different Fecundity.** *Frontiers in Physiology* 2017, **8**. <https://pubmed.ncbi.nlm.nih.gov/29326596/> PMID: 29326596 PMCID: PMC5736872
20. Chen S, Zhou Y, Chen Y, Jia G: **fastp: an ultra-fast all-in-one FASTQ preprocessor.** *Bioinformatics* 2018, **34**(17):i884-i890. <https://pubmed.ncbi.nlm.nih.gov/30423086/> PMID: 30423086 PMCID: PMC6129281
21. Langmead B, Salzberg SL: **Fast gapped-read alignment with Bowtie 2.** *Nature Methods* 2012, **9**(4):357–359. <https://pubmed.ncbi.nlm.nih.gov/22388286/> PMID: 22388286 PMCID: PMC3322381

22. Kim D, Langmead B, Salzberg SL: **HISAT: A fast spliced aligner with low memory requirements.** Nature Methods 2015, **12**(4). <https://pubmed.ncbi.nlm.nih.gov/25751142/> PMID: 25751142 PMCID: PMC4655817
23. Love MI, Huber W, Anders S: **Moderated estimation of fold change and dispersion for RNA-seq data with DESeq2.** Genome Biology 2014, **15**(12):550. <https://pubmed.ncbi.nlm.nih.gov/25516281/> PMID: 25516281 PMCID: PMC4302049
24. Pertea M, Pertea GM, Antonescu CM, Chang TC, Mendell JT, Salzberg SL: **StringTie enables improved reconstruction of a transcriptome from RNA-seq reads.** Nature Biotechnology 2015, **33**(3):290–295. <https://pubmed.ncbi.nlm.nih.gov/25690850/> PMID: 25690850 PMCID: PMC4643835
25. Sun L, Luo H, Bu D, Zhao G, Yu K, Zhang C, Liu Y, Chen R, Zhao Y: **Utilizing sequence intrinsic composition to classify protein-coding and long non-coding transcripts.** Nucleic Acids Research 2013. <https://pubmed.ncbi.nlm.nih.gov/23892401/> PMID: 23892401 PMCID: PMC3783192
26. Kong L, Zhang Y, Ye ZQ, Liu XQ, Zhao SQ, Wei L, Gao G: **CPC: assess the protein-coding potential of transcripts using sequence features and support vector machine.** Nucleic Acids Res 2007, **35**(Web Server issue):W345-349. <https://pubmed.ncbi.nlm.nih.gov/17631615/> PMID: 17631615 PMCID: PMC1933232
27. Mistry J, Bateman A, Finn RD: **Predicting active site residue annotations in the Pfam database.** BMC bioinformatics 2007, **8**:298. <https://pubmed.ncbi.nlm.nih.gov/17688688/> PMID: 17688688 PMCID: PMC2025603
28. Wang L, Park HJ, Dasari S, Wang S, Kocher JP, Li W: **CPAT: Coding-Potential Assessment Tool using an alignment-free logistic regression model.** Nucleic Acids Res 2013, **41**(6):e74. <https://pubmed.ncbi.nlm.nih.gov/23335781/> PMID: 23335781 PMCID: PMC3616698
29. Griffiths-Jones S, Grocock RJ, Dongen SV, Bateman A, Enright AJ: **miRBase: microRNA sequences, targets and gene nomenclature.** 2006. <https://pubmed.ncbi.nlm.nih.gov/16381832/> PMID: 16381832 PMCID: PMC1347474
30. Robinson MD, McCarthy DJ, Smyth GK: **edgeR: a Bioconductor package for differential expression analysis of digital gene expression data.** Biogeosciences 2010, **26**:139–140. <https://pubmed.ncbi.nlm.nih.gov/19910308/> PMID: 19910308 PMCID: PMC2796818
31. Wang J, Cao Y, Lu X, Wang X, Kong X, Bo C, Li S, Bai M, Jiao Y, Gao H *et al*: **Identification of the Regulatory Role of lncRNA SNHG16 in Myasthenia Gravis by Constructing a Competing Endogenous RNA Network.** Molecular therapy Nucleic acids 2020, **19**:1123–1133. <https://pubmed.ncbi.nlm.nih.gov/32059338/> PMID: 32059338 PMCID: PMC7016163
32. Liang R, Han B, Li Q, Yuan Y, Li J, Sun D: **Using RNA sequencing to identify putative competing endogenous RNAs (ceRNAs) potentially regulating fat metabolism in bovine liver.** Scientific reports 2017, **7**(1):6396. <https://pubmed.ncbi.nlm.nih.gov/28743867/> PMID: 28743867 PMCID: PMC5527063
33. Zuo J, Wang Y, Zhu B, Luo Y, Wang Q, Gao L: **Analysis of the Coding and Non-Coding RNA Transcriptomes in Response to Bell Pepper Chilling.** International journal of molecular sciences 2018,

- 19(7). <https://pubmed.ncbi.nlm.nih.gov/29987249/> PMID: 29987249 PMCID: PMC6073856
34. Xu XW, Zhou XH, Wang RR, Peng WL, An Y, Chen LL: **Functional analysis of long intergenic non-coding RNAs in phosphate-starved rice using competing endogenous RNA network.** *Scientific Reports* 2016, **6**:20715. <https://pubmed.ncbi.nlm.nih.gov/26860696/> PMID: 26860696 PMCID: PMC4748279
35. Qiang Q, Zhang G, Tao M, Qian W, Wang J, Ye Z, Cao C, Hu Q, Kim J, Larkin DM: **Supplementary information for: The yak genome and adaptation to life at high-altitude.** <https://pubmed.ncbi.nlm.nih.gov/22751099/> PMID: 22751099
36. Rodgers RJ, Irving-Rodgers HF: **Formation of the Ovarian Follicular Antrum and Follicular Fluid.** *Biology of Reproduction* 2010, **82**(6):1021–1029. <https://pubmed.ncbi.nlm.nih.gov/20164441/> PMID: 20164441
37. Eppig JJ, Chesnel F, Hirao Y, O'Brien MJ, Wigglesworth K: **Oocyte control of granulosa cell development: how and why.** *Human Reproduction* 1997, **12**(11 Suppl):127–132. <https://pubmed.ncbi.nlm.nih.gov/9433969/> PMID: 9433969
38. Sammad A, Hu L, Luo H, Abbas Z, Umer S, Zhao S, Xu Q, Khan A, Wang Y, Zhu H *et al.* **Investigation of Metabolome Underlying the Biological Mechanisms of Acute Heat Stressed Granulosa Cells.** *International journal of molecular sciences* 2022, **23**(4). <https://pubmed.ncbi.nlm.nih.gov/35216260/> PMID: 35216260 PMCID: PMC8879866
39. Su YQ: **Mouse Oocyte Control of Granulosa Cell Development and Function: Paracrine Regulation of Cumulus Cell Metabolism.** *Seminars in Reproductive Medicine* 2009. <https://pubmed.ncbi.nlm.nih.gov/19197803/> PMID: 19197803 PMCID: PMC2742468
40. Conti M, Hsieh M, Zamah AM, Oh JS: **Novel signaling mechanisms in the ovary during oocyte maturation and ovulation.** *Molecular & Cellular Endocrinology* 2012, **356**(1–2):65–73. <https://pubmed.ncbi.nlm.nih.gov/22101318/> PMID: 22101318 PMCID: PMC4104635
41. Amireault, P: **Intracellular cAMP and calcium signaling by serotonin in mouse cumulus-oocyte complexes.** *Molecular Pharmacology* 2005, **68**(6):1678–1687. <https://pubmed.ncbi.nlm.nih.gov/16131615/> PMID: 16131615
42. Wigglesworth K, Lee KB, O'Brien MJ, Peng J, Matzuk MM, Eppig JJ: **Bidirectional communication between oocytes and ovarian follicular somatic cells is required for meiotic arrest of mammalian oocytes.** *Proceedings of the National Academy of Sciences of the United States of America* 2013, **110**(39):E3723–E3729. <https://pubmed.ncbi.nlm.nih.gov/23980176/> PMID: 23980176 PMCID: PMC3785791
43. Fuente RDL, Eppig JJ: **Transcriptional activity of the mouse oocyte genome: companion granulosa cells modulate transcription and chromatin remodeling.** *Developmental Biology* 2001, **229**(1):224–236. <https://pubmed.ncbi.nlm.nih.gov/11133166/> PMID: 11133166
44. Matzuk MM, Burns KH, Viveiros MM, Eppig JJ: **Intercellular Communication in the Mammalian Ovary: Oocytes Carry the Conversation.** *Science* 2002, **296**(5576):2178–2180. <https://pubmed.ncbi.nlm.nih.gov/12077402/> PMID: 12077402

45. Lv X, He C, Huang C, Wang H, Hua G, Wang Z, Zhou J, Chen X, Ma B, Timm BK: **Timely expression and activation of YAP1 in granulosa cells is essential for ovarian follicle development.** *The FASEB Journal*, **33**(9). <https://pubmed.ncbi.nlm.nih.gov/31199671/> PMID: 31199671 PMCID: PMC6704445
46. Vanderhyden BC, Telfer EE, Eppig JJ: **Mouse oocytes promote proliferation of granulosa cells from preantral and antral follicles in vitro.** *Biology of Reproduction* 1992, **46**(6):1196–1204. <https://pubmed.ncbi.nlm.nih.gov/1391318/> PMID: 1391318
47. Russell MC, Cowan RG, Harman RM, Walker AL, Quirk SM: **The Hedgehog Signaling Pathway in the Mouse Ovary.** *Biology of Reproduction* 2007, **77**(2):226. <https://pubmed.ncbi.nlm.nih.gov/17392501/> PMID: 17392501
48. Warma A, Lussier JG, Ndiaye K: **Tribbles Pseudokinase 2 (TRIB2) Regulates Expression of Binding Partners in Bovine Granulosa Cells.** *International journal of molecular sciences*, **22**(4):1533. <https://pubmed.ncbi.nlm.nih.gov/33546420/> PMID: 33546420 PMCID: PMC7913596
49. Schlessinger K, Hall A, Tolwinski N: **Wnt signaling pathways meet Rho GTPases.** *Genes & development* 2009, **23**(3):265–277. <https://pubmed.ncbi.nlm.nih.gov/19204114/> PMID: 19204114
50. Bonnet A, Cabau C, Bouchez O, Sarry J, Marsaud N, Foissac S, Woloszyn F, Mulsant P, Mandonpepin B: **An overview of gene expression dynamics during early ovarian folliculogenesis: specificity of follicular compartments and bi-directional dialog.** *Bmc Genomics* 2013, **14**(1):904–904. <https://pubmed.ncbi.nlm.nih.gov/24350644/> PMID: 24350644 PMCID: PMC3890531
51. Wang K, Liu CY, Zhou LY, Wang JX, Wang M, Zhao B, Zhao WK, Xu SJ, Fan LH, Zhang XJ: **APF lncRNA regulates autophagy and myocardial infarction by targeting miR-188-3p.** *Nature Communications* 2015, **6**:6779. <https://pubmed.ncbi.nlm.nih.gov/25858075/> PMID: 25858075
52. Ying, Huang: **The novel regulatory role of lncRNA-miRNA-mRNA axis in cardiovascular diseases.** *Journal of cellular and molecular medicine* 2018. <https://pubmed.ncbi.nlm.nih.gov/30188595/> PMID: 30188595 PMCID: PMC6237607
53. Schmitz SU, Grote P, Herrmann BG: **Mechanisms of long noncoding RNA function in development and disease.** *Cellular and Molecular Life Sciences* 2016, **73**(13):2491–2509. <https://pubmed.ncbi.nlm.nih.gov/27007508/> PMID: 27007508 PMCID: PMC4894931
54. Sherr CJ, Roberts JM: **Living with or without cyclins and cyclin-dependent kinases.** *Genes & Development* 2004, **18**(22):2699–2711. <https://pubmed.ncbi.nlm.nih.gov/15545627/> PMID: 15545627
55. Sekulic A, Haluska P, Miller AJ, De Lamo JG, Ejadi S, Pulido JS, Salomao DR, Thorland EC, Vile RG, Swanson DL: **Malignant melanoma in the 21st century: the emerging molecular landscape.** *Mayo Clinic Proceedings* 2008, **83**(7):825–846. <https://pubmed.ncbi.nlm.nih.gov/18613999/> PMID: 18613999 PMCID: PMC2739389
56. Dai J, Wei RJ, Li R, Feng JB, Liu PS: **A study of CCND1 with epithelial ovarian cancer cell proliferation and apoptosis.** *European Review for Medical & Pharmacological Sciences* 2016, **20**(20):4230. <https://pubmed.ncbi.nlm.nih.gov/27831653/> PMID: 27831653

57. Yue, Xiong, Hannon, Gregory, J., Hui, Zhang, Casso, David, Kobayashi: **P21 is a universal inhibitor of cyclin kinases.** *Nature* 1993. <https://pubmed.ncbi.nlm.nih.gov/8259214/> PMID: 8259214
58. Labaer J, Garrett M, Stevenson LF, Slingerland JM, Sandhu C, Chou HS, Fattaey A, Harlow E: **New functional activities for the p21 family of CDK inhibitors.** *Genes & Development* 1997, **11**(7):847. <https://pubmed.ncbi.nlm.nih.gov/9106657/> PMID: 9106657
59. Dash, Bipin, C., El-Deiry, Wafik, S.: **Phosphorylation of P21 in G2/M Promotes Cyclin B-Cdc2 Kinase Activity.** *Molecular & Cellular Biology* 2005, **25**(8):3364–3387. <https://pubmed.ncbi.nlm.nih.gov/15798220/> PMID: 15798220 PMCID: PMC1069593
60. Bunz, F.: **Requirement for p53 and p21 to Sustain G2 Arrest After DNA Damage.** *Science* 1998, **282**(5393):1497–1501. <https://pubmed.ncbi.nlm.nih.gov/9822382/> PMID: 9822382
61. Song S, Zhang J, Su Q, Zhang W, Zhuang W: **Downregulation of ITGA6 confers to the invasion of multiple myeloma and promotes progression to plasma cell leukaemia.** *British Journal of Cancer.* <https://pubmed.ncbi.nlm.nih.gov/33785876/> PMID: 33785876 PMCID: PMC8144434

Additional File 1

Additional File 1 is not available with this version.

Figures

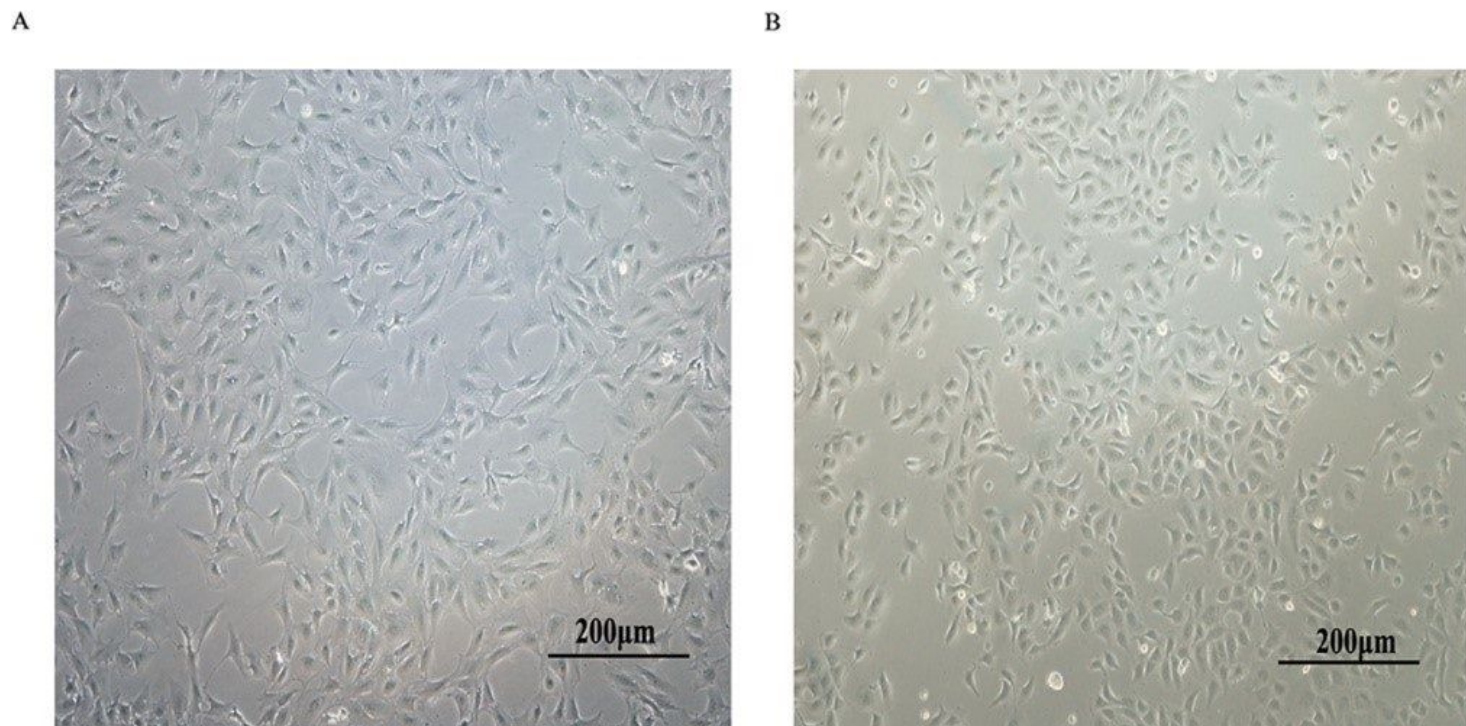


Figure 1

Primary culture of granulosa cells and cumulus cells (10^x magnification). (A) Granulosa cells; (B) Cumulus cells.

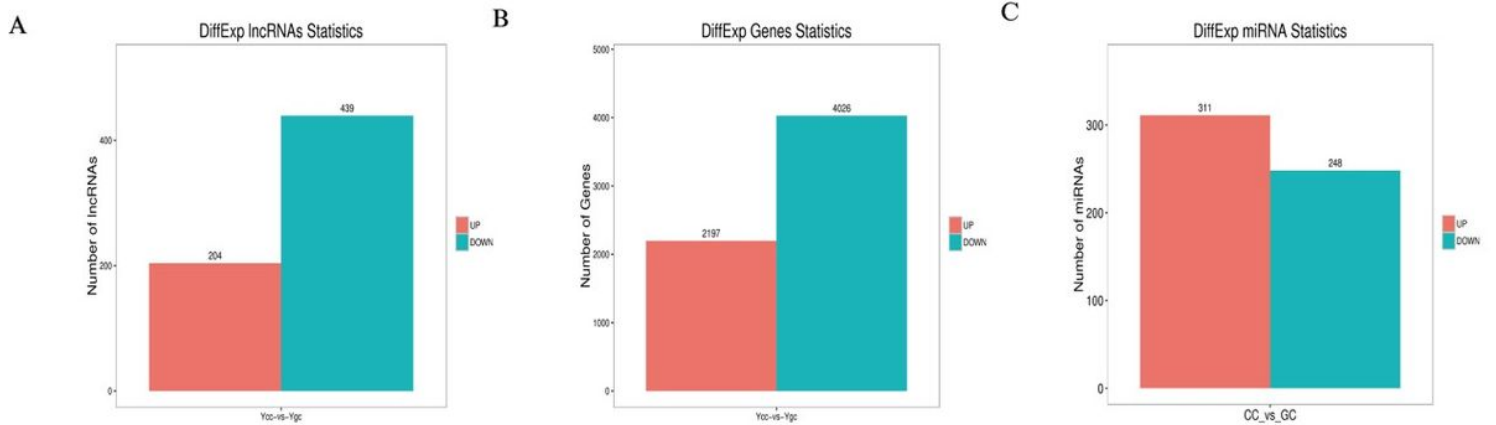


Figure 2

Different genes of upregulation and downregulation. (A) IncRNA; (B) mRNA; (C) miRNA.

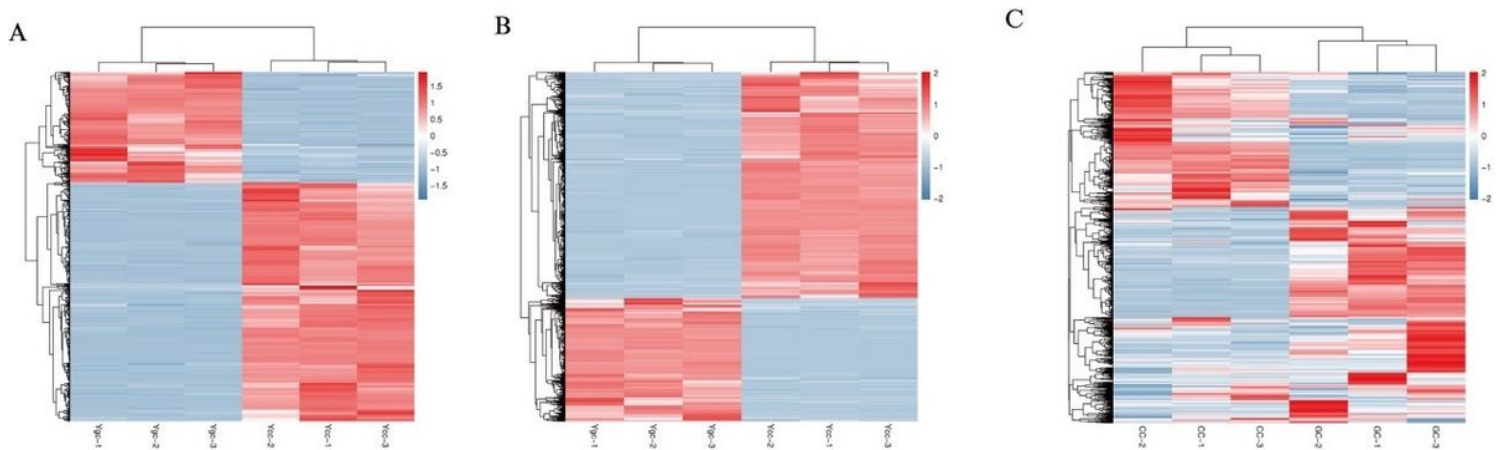


Figure 3

Each column represents a sample, and each row represents a IncRNA. The expression level of IncRNA in different samples is represented by different colors. The redder the color, the higher expression level, and the bluer the color, the lower the expression level. Gene expression number and profiling analyses of differentially expressed IncRNA and mRNA among CC and GC. (A) Heat map of the DE IncRNAs; (B) Heat map of the DE mRNAs; (C) Heat map of the DE miRNAs.

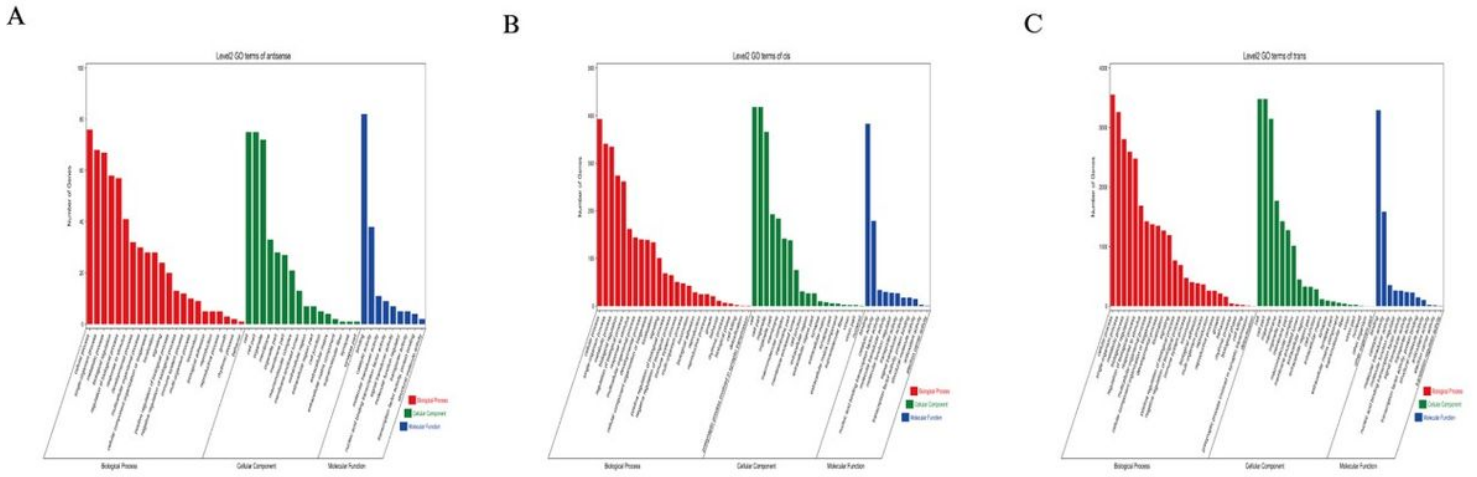


Figure 4

GO functional annotation histogram of the candidate genes related to DE lncRNAs and DE mRNAs.

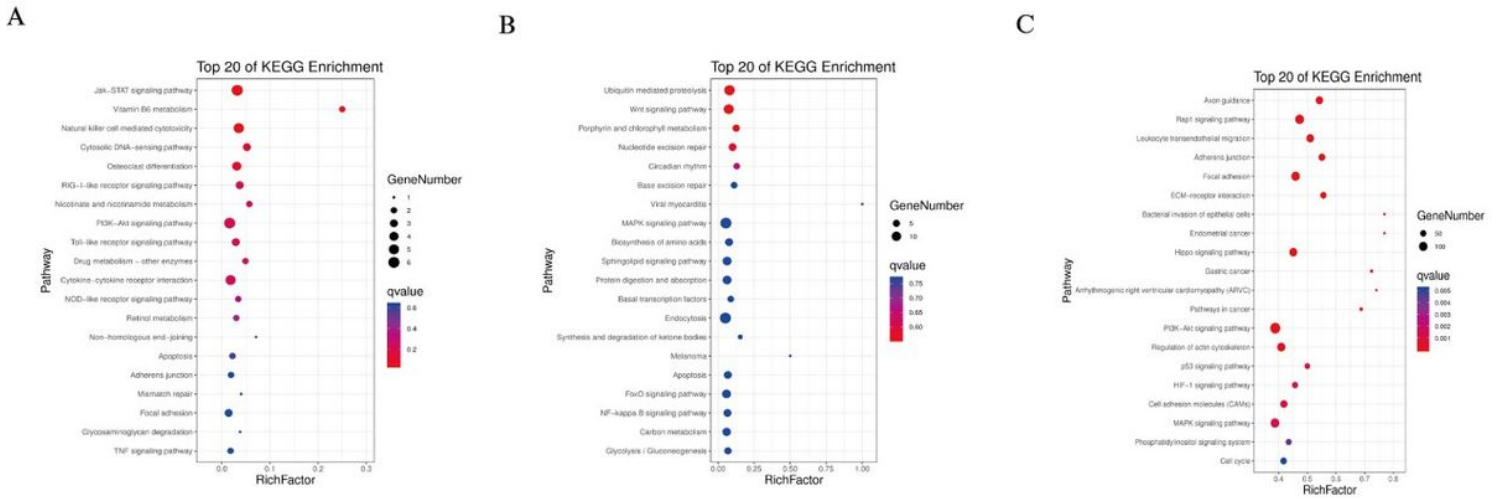
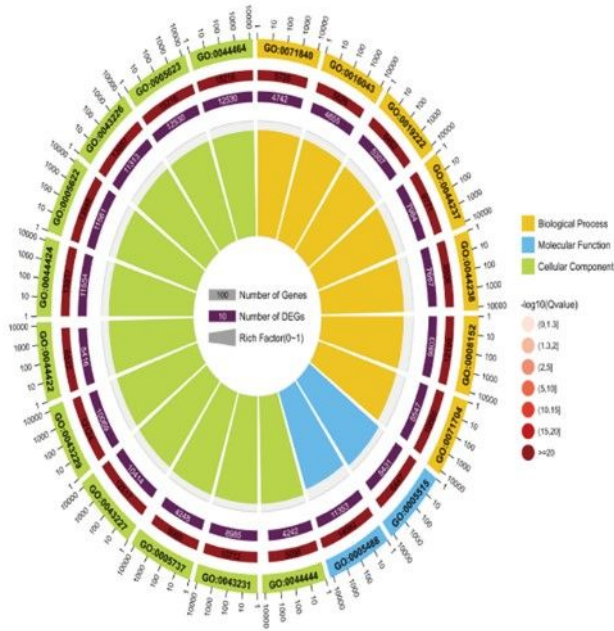
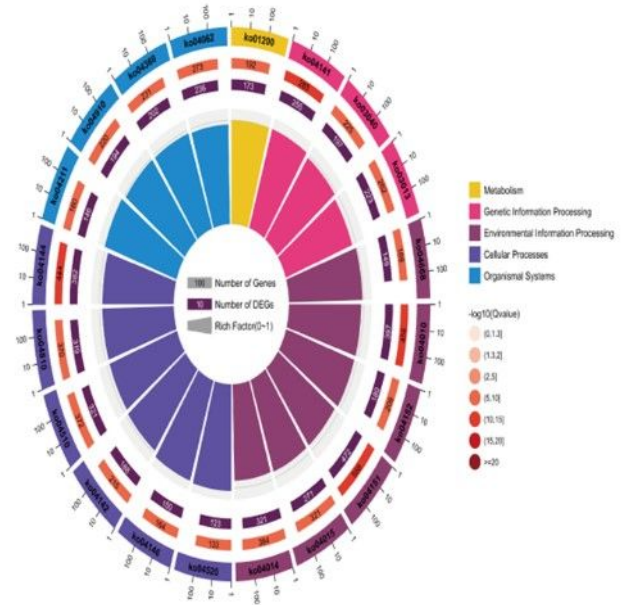


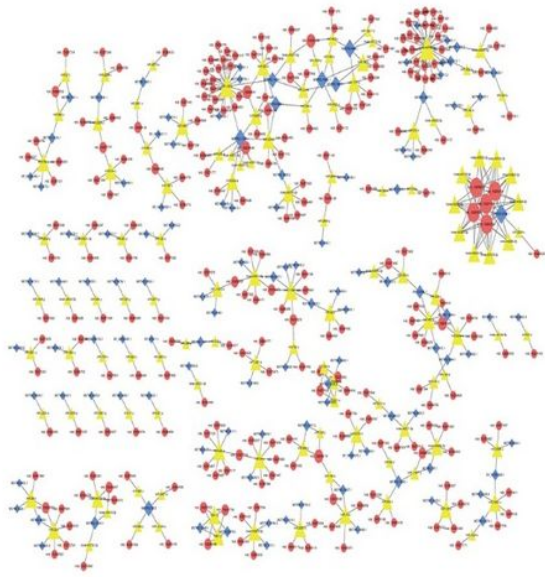
Figure 5

KEGG pathway assessment of the source genes of differential top 20 lncRNAs and mRNAs.

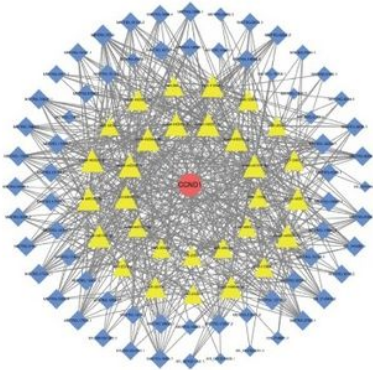
A**B****Figure 6**

Radar map representations of the target genes of differential miRNAs. **(A)** GO functional annotation. **(B)** KEGG pathway assessment.

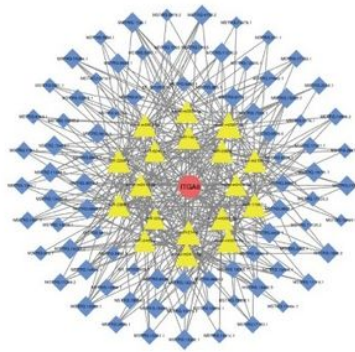
A



B



C



D

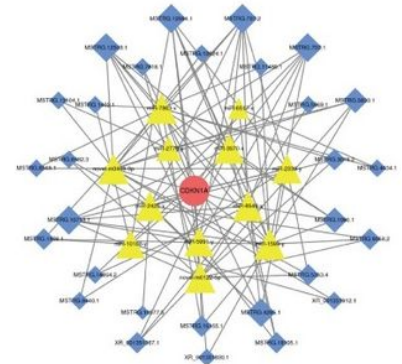
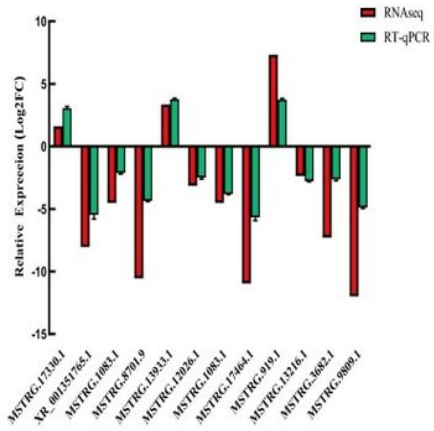


Figure 7

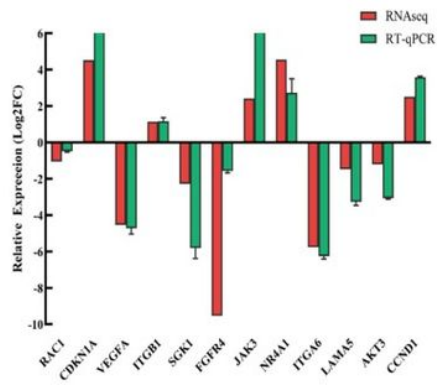
(A) CeRNA regulatory network in cumulus cells and granulosa cells in yak ovary; (B) Subnetwork of MSTRG.13544.2-miR-221-x|miR-2357-x|miR-338-y|novel-m0707-5p-ncbi_102270546 (CCND1); (C) MSTRG.9576.6-miR-11987-x|miR-2284-y|novel-m0070-3p|novel-m0191-3p-ncbi_102265941 (ITGA6); (D) MSTRG.5969.1-novel-m0122-5p|novel-m0468-3p-ncbi_102268672 (CDKN1A).

The diamond: LncRNAs. The triangles: miRNAs. The circles: mRNAs.

A



B



C

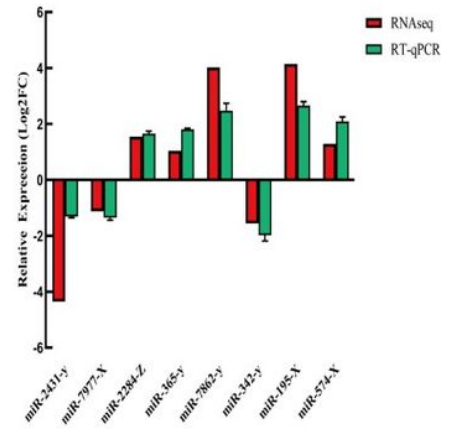


Figure 8

Comparison of the gene expression levels determined by RNA-seq and RT-qPCR. (A) DE lncRNAs; (B) DE mRNAs; (C) DE miRNAs.